Sādhanā Vol. 39, Part 5, October 2014, pp. 1245–1257. © Indian Academy of Sciences

Experimental studies of local scour in the pressurized OCF below a wooden log across the flow

SOUMEN MAJI, PRASHANTH REDDY HANMAIAHGARI* and SUBHASISH DEY

Department of Civil Engineering, Indian Institute of Technology Kharagpur, Kharagpur, 721 302, India
e-mail: hpr@civil.iitkgp.ernet.in

MS received 23 September 2013; revised 11 March 2014; accepted 26 April 2014

Abstract. The proposed study examined and reviewed the published experimental results related to clear water scour below a cylinder across the flow. It also highlighted the limitations of existing methods for estimating the scour depth below a submerged cylinder. In the present study, experiments were performed for 50% and 75% submergences of a 70 mm diameter cylinder in the free surface flow over a uniform sand bed with $d_{50} = 0.98$ mm downstream of an apron. Based on the experimental results, an empirical equation was proposed to estimate the amount of gap flow between the cylinder and the bed for an equilibrium scour for a given flow depth and sediment properties. Measured scour profile consisted of a scour hole and immediately followed by a dune. However, no general sediment transport was occurring away from the cylinder due to the undisturbed bed shear stress less than or equal to the critical shear stress required for the sediment entrainment. Different submergence ratios of the cylinder resulted in different longitudinal and vertical extensions of the scour hole and the dune. The maximum equilibrium scour depth occurred when the cylinder is fully submerged in the unidirectional flow with water depth equals to the cylinder diameter. The non-dimensional measured scour profiles were found to be similar. The characteristic lengths of the scour hole and the dune were computed analytically by approximating the measured scour profile by third degree polynomials. The computed non-dimensional scour profiles compared satisfactorily with the measured profiles. It was found that analytical non-dimensional scour profiles were identical for a given diameter of a cylinder with different submergences for the same flow conditions.

Keywords. Scour depth; dune; submerged pipelines; open channel flow (OCF); sediment transport; bed shear stress.

*For correspondence

1. Introduction

Scour is the natural occurrence of lowering the level of riverbeds by erosive action of open channel flow (OCF) due to an obstruction in the flow field. Interactions between the fallen tree across the flow and an erodible bed tend to cause local scouring around the tree. The problem is similar to local scour below pipelines laid across on the river/sea beds to convey water, oil, gas, or any fluid, commonly occurs by the erosive action of current. For example, scour below existing operational subsea oil pipelines between Norway and United Kingdom. Due to its practical importance, extensive research is directed to better understand the scour under the submerged pipelines. Scour underneath the pipeline may expose part of the pipe to be suspended in water. If the free span of the pipe is long enough, the pipe may experience resonant flow-induced oscillations due to wake vortex shedding leading to structural failure. Therefore, an accurate estimation of the scour depth is very important in the design of submarine pipeline. At present, several empirical methods based on various research findings are available in the literature for estimating the equilibrium scour depth under unidirectional current. The present study investigated the development of the scour hole in a cohesionless uniform sediment bed below a floating wooden cylinder subjected to different submergence ratios. The experimental results are used to describe the similarity of the non-dimensional measured scour profiles and the influences of various parameters on scour depth.

2. Literature review

One of the most important aspects in pipeline design is the prediction of the vertical and lateral extent of scour below the pipeline. A literature review reveals that Chao & Hennessy (1972) developed an analytical model to predict maximum local scour below pipelines based on potential flow theory. Kjeldsen *et al* (1973) studied scour below pipelines in live-bed condition and they found that scour depth (d_s) is a function of the approach flow velocity (U) and pipe diameter. Mao (1986) identified two cases of the scouring process, namely the jet period, which decides the maximum scour depth d_s and wake period (which decides the location of maximum scour depth). Hansen *et al* (1986) calculated the flow field and scour profiles by using the modified Von Müller method and integrating the sediment continuity equation respectively. Ibrahim & Nalluri (1986) also stated that the scour depth is related to flow velocity and pipe diameter, besides, influence of flow depth was also included in their analysis. Chiew (1990) identified that piping plays a dominant role in initiating scour at submarine pipelines. Chiew (1991), Sumer & Fredsøe (1992), and Whitehouse (1998) comprehensively reviewed the ongoing research on scour below pipelines. They excluded the effect of flow depth (h) and sediment size. In addition, Chiew (1991) proposed an iterative method for the estimation of scour depth (d_s) based on the experimental data. Li and Cheng (1999) used the finite difference method to solve the Laplace equation of velocity potential and a boundary adjustment technique to calculate the equilibrium scour profiles below pipelines. Brørs (1999) used the finite element method to simulate the scour profiles underneath of offshore pipelines. Dey & Singh (2008) observed that the equilibrium scour depth increases with increase in approach flow depth for shallow flow depths and it is not influenced by the high flow depths greater than five times the pipe diameter. But, in their presentation, they did not consider the dune portion in non-dimensional scour profile. Sumer & Fredsøe (2002), Cheng *et al* (2009) and Wu & Chiew (2012) have mainly studied the lateral propagation of the scour hole along the submerged pipeline under a unidirectional current in clear-water conditions. None of the aforementioned studies systematically studied the effects

of various parameters such as cylinder diameter, percentage of submergence, flow depth and gap width on the scour depth d_s which is the most important factor contributing to the pipeline failures. The present study aims at an experimental investigation of clear-water scour in the uniform sediment bed below a wooden cylinder at different floating conditions in the steady flow. The experimental results were used to describe the similarity of the equilibrium scour profiles and the influences of the above mentioned parameters on equilibrium scour depth below a circular wooden cylinder.

3. Experimental set-up and procedure

Experiments were carried out in a glass-walled rectangular horizontal flume with dimensions of 12.0 m long, 0.61 m wide and 0.70 m deep, in the hydraulic and water resources engineering laboratory at Indian Institute of Technology (IIT) Kharagpur. An adjustable tail gate was used to control the tailwater depth at the downstream end of the flume. The recirculated water supply system consisted of a constant head inlet tank, pumps and an underground reservoir. The upstream end of the flume was connected to the inlet tank and water flows into the flume through the stilling basin and a calibrated V-notch. The sediment recess is 2.40 m long, 0.60 m wide and 0.30 m deep and was filled with the uniform sediment with diameter $d_{50} = 0.98$ mm. The measured standard deviation of the sand is less than 1.4 in accordance with Dey (1996). The length and depth of sediment recess were chosen according to the expected dimensions of the equilibrium scour profiles for the maximum discharge and the minimum apron length. In order to assert the same bed level of the sediment in the recess, an apron was made at an elevation of 0.30 m from the flume bottom throughout the upstream length of the flume. A schematic diagram of the experimental set-up is shown in figure 1. Two small outlets were provided at the bottom of the downstream wall of the sediment recess to drain the water from the sediment bed at the end of the experiment. A sediment trap of 0.6 m long was provided at the downstream end of sediment recess to arrest the scoured sediment. The diameter and length of the wooden cylinder were 70 mm and 0.60 m respectively. The cylinder was rigidly held at any floating condition by hanging supports at both the ends. Photographs of experimental set-up before starting the experiment are shown in figure 2.

The flume was slowly filled with water at a low rate by carefully opening the inlet valve to prevent the undesirable scour of sediment bed during the initial stage. The experiment was started by regulating the discharge to a required value. A required water depth was achieved

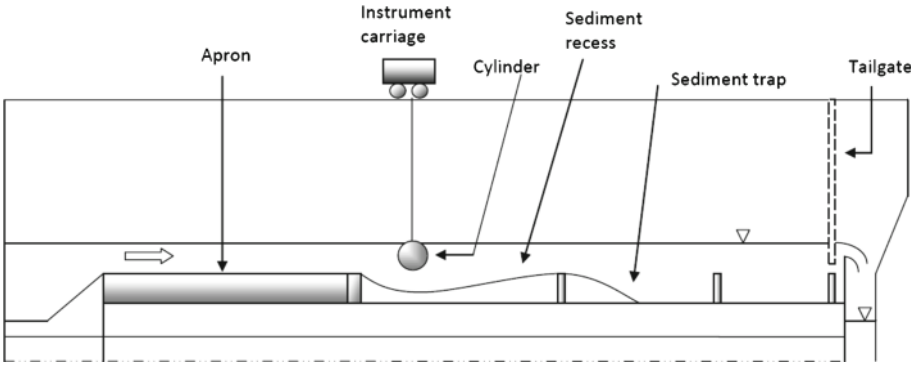

Figure 1. Schematic of the experimental set-up.

Figure 2. Photographs of experimental set-up before starting the experiment; (**a**) viewing from upstream and (**b**) viewing from downstream.

by controlling the tail water depth. Minimum duration of each experiment was between two to three hours to ensure that the equilibrium scour depth was reached. During the experiments, the average approach flow velocity U was maintained at approximately 80% of the critical velocity U_C of the uniform sediment bed to satisfy the nearly limiting clear-water condition. Following a semi-logarithmic empirical equation was proposed in this paper to compute critical velocity U_C, which is dependent on approach flow depth (h), and corresponding gap flow through the scour hole may be computed.

$$\frac{U_C}{U_{*C}} = 5.75 \log_{10}\left(\frac{h}{2d_{50}}\right) + 6, \tag{1}$$

where U_{*C} = critical shear velocity of sediment which was calculated from the Shields diagram by using Van Rijn (1984) empirical equation of the shield curve. Average approach flow velocity was obtained from the Eq. (1) and corresponding flow discharge was maintained in the flume using the calibrated V-notch. The water level above the crest of V-notch was measured by a Vernier point gauge with an accuracy of $\pm$ 0.1 mm.

The hydrodynamics and mode of sediment transport in an evolving scour hole change considerably due to the complex interaction of the flow with floating wooden cylinder. In the initial stage, the suspension of sediments was the only means of sediment transport. Scour initiates below the cylinder when the bed shear stress exerted by the flow exceeds the critical bed shear stress of the bed sediments. The upstream portion of the scour hole develops a steep slope and an irregularity in the profile between arises due to backward rolling movement of particles along the upstream slope due to the turbulence. Photographs of scoured bed are shown in figure 3. As the geometry of scour hole progresses with time, the temporal evolution of scour profiles at different time intervals were recorded on a thin transparent plastic sheet which is attached to the outer side of glass side wall of the flume. It was observed that the rate of scouring is very high during the initial stage, however, it gradually decreased as time elapsed. Ultimately, the equilibrium scour profile was reached when there is no sediment movement in the location of maximum scour. The time required to reach the equilibrium scour profile was recorded for each experimental run.

Figure 3. Bed scour after an experiment; (**a**) viewed from downstream and (**b**) viewed from a side.

Before the start of each run, the disturbed bed was levelled after the dewatering and drying the bed. The whole procedure was then repeated and the new set of scour profiles was obtained.

4. Results and discussion

In the present experiments, approach flow velocity was maintained at 0.8 times the critical shear velocity for a given flow depth. The clear water flow velocity was computed as 0.270 m/s using Eq. (1) for a flow depth of 70 mm. Scour profiles were mapped at different time intervals for 50% and 70% of submergences of 70 mm diameter cylinder for the above mentioned flow conditions. The measured scour profiles consist of a scour hole below the cylinder and followed by a dune. Therefore, the existence of similarity of the scour profiles was established by plotting the scour profiles in non-dimensional coordinates $(\hat{x}, \hat{y})$, where $\hat{x}$ is x/d_s and $\hat{y}$ is y/d_s where x is the horizontal distance, y is the vertical distance and d_s is the maximum scour depth at any time t. The non-dimensional scour profile follows a definite pattern as shown in figure 4. Figure 5a

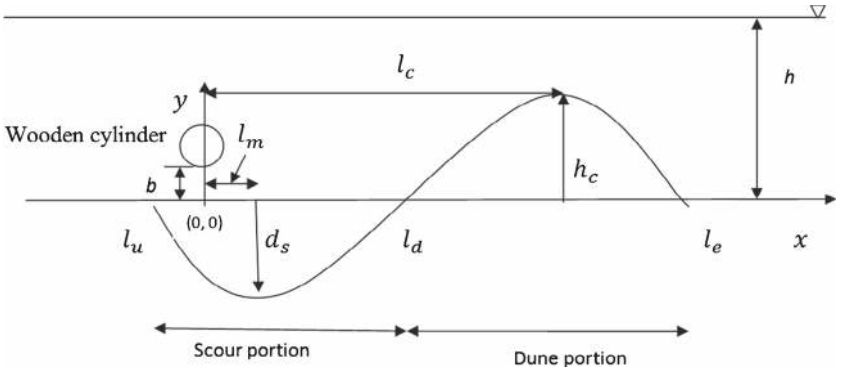

Figure 4. Non-dimensional plot of equilibrium scour profiles.

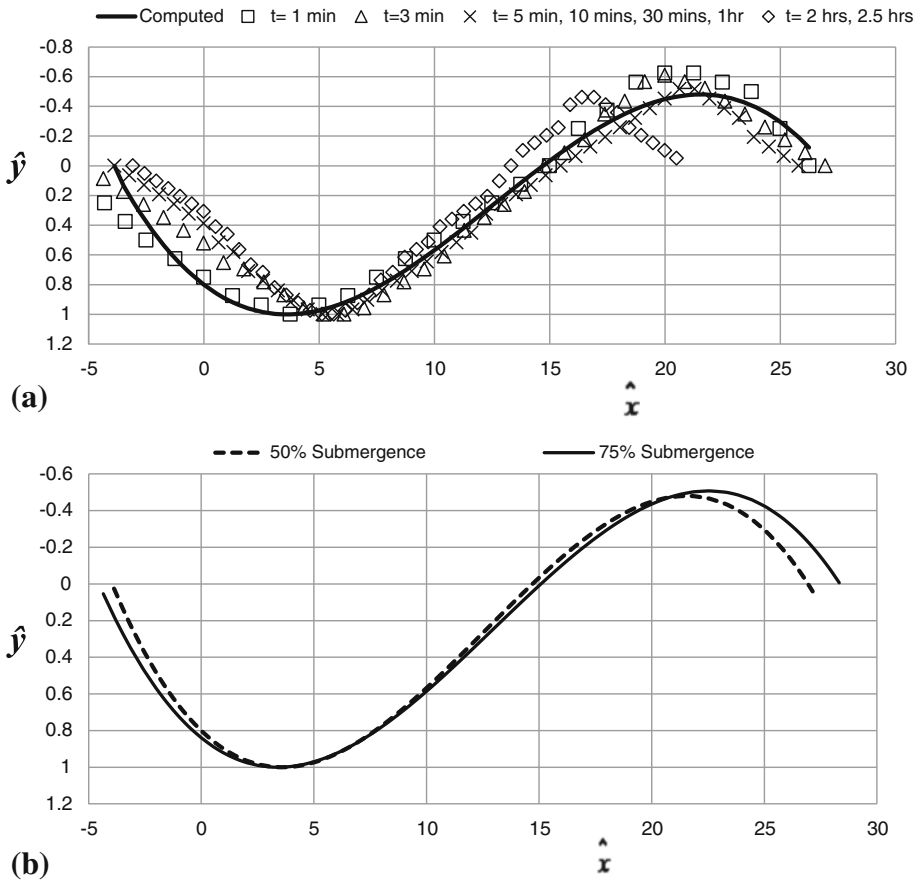

Figure 5. (**a**) Non-dimensional scour profiles at different time intervals due to 70 mm cylinder with 50% submerged. (**b**) Computed non-dimensional scour profiles for 75% and 50% submergences of 70 mm diameter cylinder.

shows the non-dimensional measured scour profiles at different time intervals, which indicates the similarity of the profiles of scour hole and downstream dune, as obtained by Rajaratnam (1981), Ali & Lim (1986), Dey & Westrich (2003), and Dey & Sarkar (2006). Furthermore, the non-dimensional scour profiles were essentially represented by following two polynomials (Eqs. 2 and 3), each for scour hole and dune, respectively.

$$\hat{y}\left(\hat{y} \leq 0\right) = a_0 + a_1\hat{x} + a_2\hat{x}^2 + a_3\hat{x}^3 \tag{2}$$

$$\hat{y}\left(\hat{y} \geq 0\right) = b_0 + b_1\hat{x} + b_2\hat{x}^2 + b_3\hat{x}^3, \tag{3}$$

where a_{0-3} and b_{0-3} are coefficients. The coefficients a_0, a_1, a_2 and a_3 were determined using the scour profile characteristics as given below.

$$x = l_u,\ y = 0;\ \text{then}\ 0 = a_0 + a_1\left(-\alpha_1\right) + a_2\left(\alpha_1\right)^2 + a_3\left(\alpha_1\right)^3, \tag{4a}$$

$$x = l_d,\ y = 0;\ \text{then}\ 0 = a_0 + a_1\alpha_2 + a_2\left(\alpha_2\right)^2 + a_3\left(\alpha_2\right)^3, \tag{4b}$$

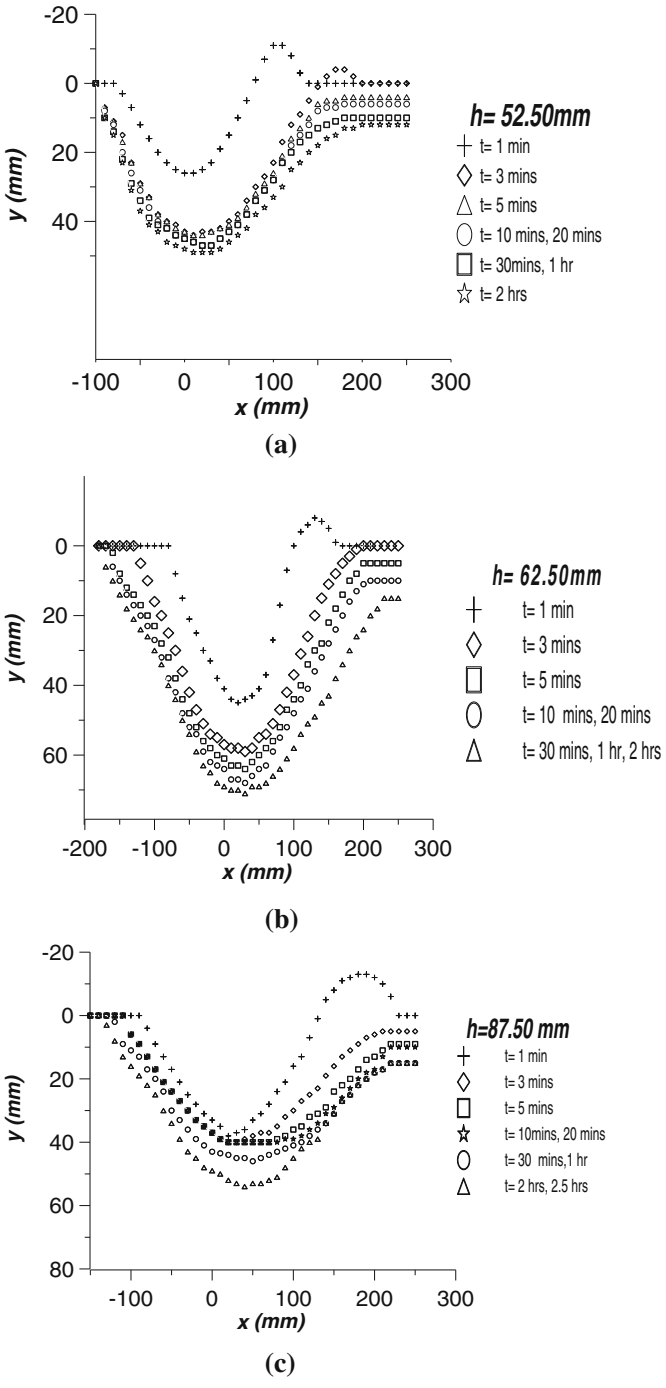

Figure 6. (**a**) Scour profiles with time when wooden cylinder touches sediment bed and velocity of flow was 0.255 m/s. (**b**) Scour profiles with time when wooden cylinder was 10 mm above the sediment bed and velocity of flow was 0.263 m/s. (**c**) Scour profiles with time when wooden cylinder was 35 mm above the sediment bed and velocity of flow was 0.278 m/s.

$$x = l_m, y = -d_s; \text{then} - 1 = a_0 + a_1\alpha_3 + a_2\,(\alpha_3)^2 + a_3\,(\alpha_3)^3\,, \tag{4c}$$

$$x = l_m, \frac{dy}{dx} = 0; \text{then}\, 0 = a_1 + a_2\alpha_4 + a_3\,(\alpha_4)^2\,, \tag{4d}$$

where $\alpha_1 = \frac{l_u}{d_s}$; $\alpha_2 = \frac{l_d}{d_s}$; $\alpha_3 = \frac{l_m}{d_s}$; and $\alpha_4 = \frac{x}{d_s}$; Hence, from Eq. (4a–d) the values of coefficient a_0, a_1, a_2 and a_3 were obtained. Similarly, the coefficients b_0, b_1, b_2, and b_3 of Eq. (3) were determined from following boundary conditions.

$$x = l_d, y = 0; x = l_e, y = 0; x = l_c, y = h_c; x = 0, \frac{d\,(y \le 0)}{dx} = \frac{d\,(y > 0)}{dx}. \tag{5}$$

Measured scour profiles for 50% and 75% submergences of 70 mm diameter at different time intervals have been used to get the analytical non-dimensional scour profiles corresponding to 50% and 75% submergence of 70 mm diameter. The analytical non-dimensional scour profiles of different time intervals for a given submergence were averaged to get the time averaged analytical non-dimensional scour profile for that submergence. The time averaged analytical non-dimensional scour profile was obtained by averaging the analytical non-dimensional scour profiles of 8 measured data sets at different time intervals (1, 3, 5, 10 and 30 min, 1, 2 and 2.5 h) of the same experiment. The time averaged analytical non-dimensional scour profile was compared with non-dimensional measured scour profiles at different time intervals for 50% submergence of 70 mm diameter cylinder. Analytical profile and measured profiles are in good agreement as shown in figure 5a. Analytical non-dimensional scour profiles are identical for 50% and 75% submergences of 70 mm cylinder for the same flow conditions (figure 5b). Therefore, it was concluded that time averaged analytical non-dimensional scour profiles are identical for a given diameter cylinder with different submergences for the same flow conditions.

4.1 *Time variation of scour depth*

Time variation of scour depths below 75% submerged cylinder with 70 mm diameter for various flow depths were shown in figure 6 and corresponding experimental data has been given in table 1. Figures 6a and b show that the equilibrium scour depth increased from 50 mm to 70 mm

Table 1. Experimental data of scour depth due to varying flow depths (cylinder diameter was 70 mm with 75% submergence).

U (m/s)	h (mm)	b (mm)	$\tilde{h}(h/b)$	$\tilde{d}(d_{50}/b)$	d_{se} (mm)	$\tilde{d}_{se}(d_{se}/b)$	$F_u\left(U/\sqrt{gb}\right)$	$F_0(U/\sqrt{\Delta gb})$
0.259	57.5	5	11.50	0.19	59.0	11.8	1.170	2.08
0.263	62.5	10	6.25	0.095	70.0	7.10	0.839	2.12
0.266	67.5	15	4.50	0.060	60.0	4.13	0.693	2.14
0.269	72.5	20	3.63	0.047	64.0	3.20	0.607	2.16
0.270	77.5	25	3.10	0.038	70.0	2.80	0.545	2.17
0.275	82.5	30	2.75	0.031	60.0	2.00	0.506	2.21
0.278	87.5	35	2.50	0.027	51.8	1.48	0.474	2.24
0.283	97.5	45	2.16	0.021	54.0	1.20	0.425	2.28
0.287	107.5	55	1.95	0.017	60.0	1.09	0.390	2.31
0.291	117.5	65	1.80	0.014	54.0	0.83	0.364	2.34
0.297	132.5	80	1.65	0.011	60.8	0.76	0.335	2.39
0.303	152.5	100	1.52	0.009	55.0	0.55	0.308	2.44

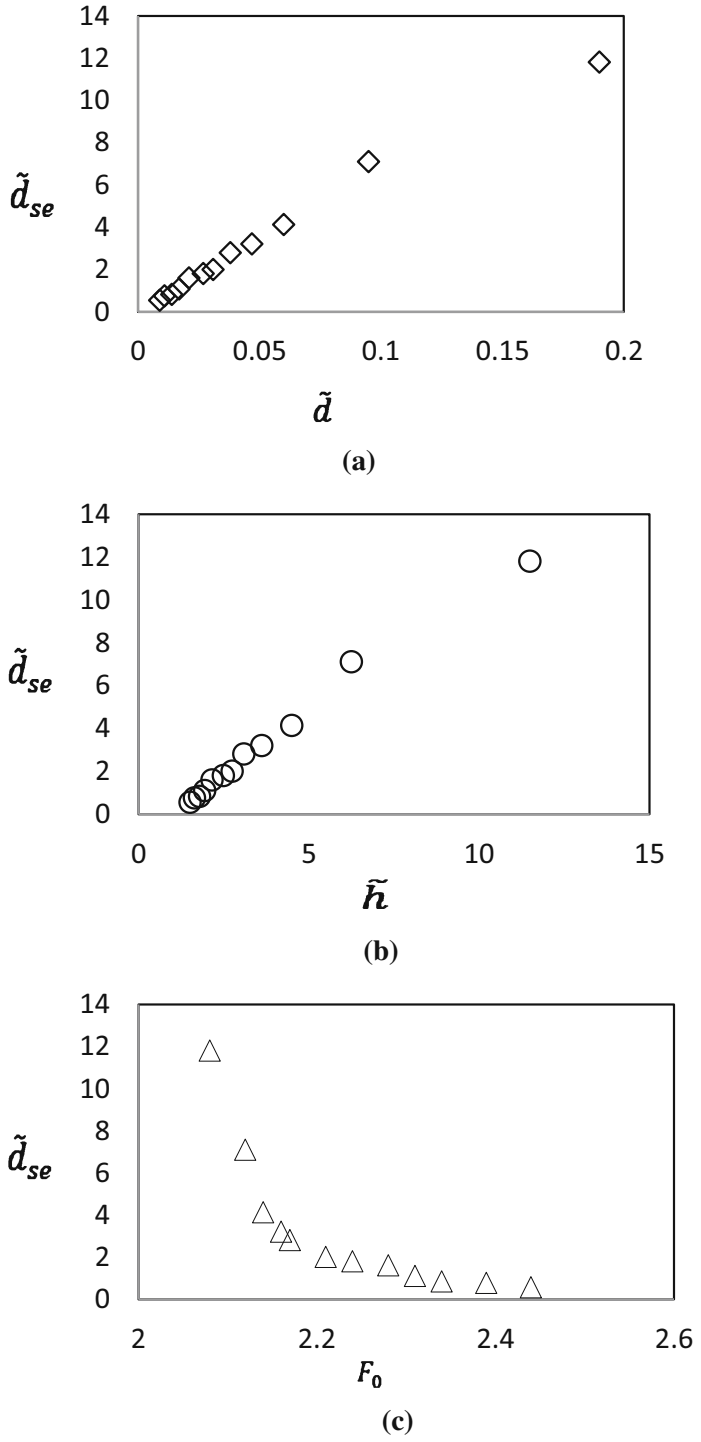

Figure 7. (**a**) Variation of $\tilde{d}_{se}$ with $\tilde{d}$. (**b**) Variation of $\tilde{d}_{se}$ with $\tilde{h}$. (**c**) Variation of $\tilde{d}_{se}$ with F_0.

Table 2. Equilibrium scour depth (d_{se}) for different submerged conditions of 70 mm diameter cylinder.

Submergence % (submerged depth in mm)	Cylinder gap opening (b) (mm)	Measured equilibrium scour depth (d_{se}) (mm)
100 (70.0)	0.0	110.0
90 (63.0)	7.0	75.0
75 (52.5)	17.5	64.0
60 (42.0)	28.0	38.0
40 (28.0)	42.0	21.0
20 (14.0)	56.0	7.0
5 (3.5)	66.5	0.0

as water depth increased from 52.5 mm to 62.5 mm. On the contrary, figures 6b and 6c show that the equilibrium scour depth decreased from 70 mm to 51.8 mm as water depth increased from 62.5 mm to 87.5 mm. As the flow depth increased gradually for 75% submerged cylinder, figures 6a–c indicated that the scour depth increases as the gap width increases and after reaching a certain gap width however scour depth decreases for further increase in gap width.

The data given in table 1 were also used to plot the non-dimensional graphs for a given submergence shown in figure 7. Figure 7a shows the variation of non-dimensional measured equilibrium scour depth $\tilde{d}_{se}$ with $\tilde{d}$ (sediment size/cylinder opening). It was observed that depth $\tilde{d}_{se}$ linearly increases with increase in $\tilde{d}$. The equilibrium scour depth d_{se} was also influenced by the tailwater depth h. From figure 7b, it was understood that the non-dimensional equilibrium scour depth $\tilde{d}_{se}$ as a function of the ratio of tailwater depth to sluice opening $\left(\tilde{h} = \frac{h}{b}\right)$ under the clear water condition, i.e., $U/U_c \approx 0.8$ of variable approach depth h. Figure 7b shows the linear relation between the equilibrium scour depth $\tilde{d}_{se}$ and the scaled tailwater depth $\tilde{h}$. Using experimental data presented in table 1, the dependency of non-dimensional equilibrium scour depth $\tilde{d}_{se}$ on densimetric Froude number F_0, under clear water condition $U/U_c \approx 0.8$ for different gap openings b was shown in figure 7c. The possible reason for the sagging nature of the curve is partially attributed to the nonlinear variation in the flow field and the change in scour depth due to changes in tailwater depths. The curve plotted between the scour depth $\tilde{d}_{se}$ and densimetric Froude number F_0 was asymptotically reaching zero for F_0 values greater than 2.4.

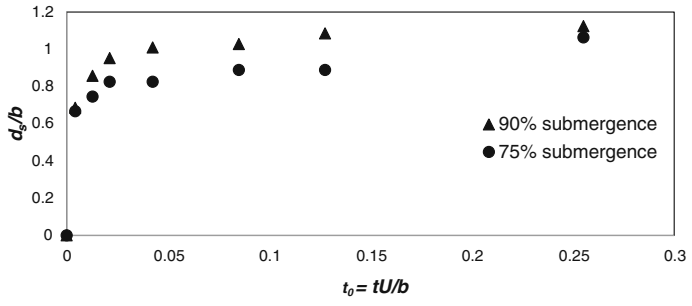

Figure 8. Variation of non-dimensional scour depth of uniform sediments for different submergence conditions.

4.2 *Effect of percentage of submergence of the cylinder on scour depth*

Cylinder with a diameter of 70 mm was kept across the flow and its percentage of submergence was changed in each experiment to study the effect of percentage of submergence of the cylinder on scour depth. Tail water depth (h) = 70 mm, velocity (U) = 0.268 m/s and flow depth = 70 mm were maintained constant in these experiments. Submerged depth of cylinder, cylinder gap opening and measured equilibrium scour depths in each experiment were presented in table 2. For water depth equal to cylinder diameter, the equilibrium scour depth reached maximum value for 100% submergence of the cylinder. Using the experimental data, the relation between non-dimensional instantaneous scour depth (d_s/b) below cylinder and non-dimensional time $\left(t_0 = \frac{tU}{b}\right)$ of scour was plotted in figure 8 for 90% and 75% submergences. Figure 8 shows that the growth rate of scour depth follows an exponential curve which is comparatively rapid in the initial stage of scouring and asymptotically reaches an equilibrium scour depth in the final stage.

5. Conclusions

The present experimental study proposed an empirical equation to determine the flowrate between cylinder and bed for the equilibrium scour for a given flow conditions and sediment properties. It was found that the equilibrium local scour profile caused by a submerged cylinder follows a definite pattern which consist a scour hole and followed by a dune. The non-dimensional equilibrium local scour profiles of scour hole and dune were expressed as polynomials and coefficients were obtained from the experimental data. The analytically computed time averaged non-dimensional scour profile was in satisfactory agreement with the non-dimensional measured profiles at different time intervals. Analytical non-dimensional scour profiles were identical for 50% and 75% submergences of 70 mm cylinder for the same flow conditions. It was concluded that the time averaged analytical non-dimensional scour profiles are identical for a given diameter cylinder with different submergences for the same flow conditions. The present research studied the variation of scour depth with time affected by 75% submergence of a cylinder with 70 mm diameter for different flow depths. It was observed that as the flow depth increased gradually for 75% submerged cylinder, scour depth increases initially as the gap width between cylinder and bed increased, after reaching a certain gap width, the scour depth decreases with further increase in gap width. The non-dimensional equilibrium scour depth linearly increases with an increase in the ratio of sediment size to gap width, and with the ratio of flow depth to gap width. The non-dimensional scour depth decreases nonlinearly with an increase in the densimetric Froude number. Present research studied the scour depth variation due to different percentages of submergence for a given flow depth. Results show an increase in the scour depth caused by an increase in submergence of the cylinder and the resulting decrease in gap width when tailwater depth equals to the cylinder diameter. The rate of scouring of sand bed below the cylinder is rapid during the initial stages, it decreases as the time progresses and asymptotically reaches an equilibrium scour profile.

Notations

a_{0-3} = Coefficient ($M^0L^0T^0$);
b = Cylinder opening (L);
b_{0-3} = Coefficient ($M^0L^0T^0$);

$\tilde{d}$ = d_{50}/b ($M^0L^0T^0$);
d_s = Maximum scour depth at time (L);
d_{se} = Maximum equilibrium scour depth (L);
$\tilde{d}_{se}$ = d_{se}/b ($M^0L^0T^0$);
d_{50} = Median sediment size (L);
F_0 = Densimetric Froude number, $U/(\Delta g d_{50})^{0.5}$ ($M^0L^0T^0$);
F_u = Jet Froude number, $U/(gb)^{0.5}$ ($M^0L^0T^0$);
g = Acceleration due to gravity (LT^{-2});
h = Tail water depth (L);
$\tilde{h}$ = h/b ($M^0L^0T^0$);
h_c = Dune height (L);
l_c = Horizontal distance of dune crest from cylinder (L);
l_e = Horizontal distance of downstream extremity of dune from cylinder (L);
l_m = Horizontal distance of maximum scour depth from cylinder (L);
l_d = Horizontal extension of scour hole from cylinder (L);
l_u = Horizontal distance scour hole starting point from cylinder (L);
s = Relative density of sediments ($M^0L^0T^0$);
t = Time of scouring (T);
U = Velocity of flow (LT^{-1});
U_c = Critical velocity (LT^{-1});
U_{*C} = Critical shear velocity (LT^{-1});
x = Horizontal distance (L);
y = Vertical distance (L);
$\hat{x}$ = x/d_s ($M^0L^0T^0$);
$\hat{y}$ = y/d_s ($M^0L^0T^0$);
Δ = $s - 1$ ($M^0L^0T^0$).

References

Ali K H M and Lim S Y 1986 Local scour caused by submerged wall jets. *Proc. Inst. Civ. Eng. London* 81(Dec): 607–645

Brørs B 1999 Numerical modeling of flow and scour at pipelines. *J. Hydraulic Eng.* 125(5): 511–523

Chao J L and Hennessy P V 1972 Local scour under ocean outfall pipe-lines. *J. Water Pollut. Control Fed.* 44(7): 1443–1447

Cheng L, Yeow K, Zhang Z and Teng B 2009 Three-dimensional scour below offshore pipelines in steady currents. *Coastal Eng.* 56(5–6): 577–590

Chiew Y M 1990 Mechanics of local scour around submarine pipe lines. *J. Hydraulic. Eng.* 116(4): 515–529

Chiew Y M 1991 Prediction of maximum scour depth at submarine pipe lines. *J. Hydraulic. Eng.* 117(4): 452–466

Dey S 1996 Sediment pick-up for evolving scour near circular cylinders. *Appl. Mathematical Modelling* 20(7): 534–539

Dey S and Sarkar A 2006 Scour downstream of an apron due to submerged horizontal jet. *J. Hydraul. Eng.* American Society of Civil Engineers (ASCE) 132(3): 246–257

Dey S and Singh N P 2008 Clear-water scour below underwater pipelines under steady flow. *J. Hydraul. Eng.* American Society of Civil Engineers (ASCE) 134(5): 588–600

Dey S and Westrich B 2003 Hydraulics of submerged jet subject to change in cohesive bed geometry. *J. Hydraul. Eng.* American Society of Civil Engineers (ASCE) 1259(1): 44–53

Hansen E A, Freds0e J and Mao Y 1986 Two-dimensional scour below pipelines. *Proc. Fifth Int. Symp. on Offshore Mech. and Arctic Eng.* American Society of Mechanical Engineers 3: 670–678

Ibrahim A and Nalluri C 1986 Scour prediction around marine pipelines. *Proc. Fifth Int. Symp. on Offshore Mech. and Arctic Eng.* American Society of Mechanical Engineers 3: 679–684

Kjeldsen S P, GjØrsvik O, Bringaker K G and Jacobsen J 1973 Local scour in offshore pipe lines. *Proceedings of the Second International Conference on Port and Ocean Engineering Under Arctic Conditions* (POAC), August 27–30, p. 308–331,

Li F and Cheng L 1999 Numerical model for local scour under offshore pipelines. *J. Hydraulic. Eng.* 125(4): 400–406

Mao Y 1986 *The interaction between a pipeline and an erodible bed*, thesis presented to the Technical University of Denmark, at Lyngby, Denmark, in partial fulfilment of the requirements for the degree of Doctor of Philosophy

Rajaratnam N 1981 Erosion by plane turbulent jets. *J. Hydraul. Res.* 19(4): 339–358

Sumer M B and Fredsøe J 1992 A review of wave/current-induced scour around pipelines. *Coastal Eng. Proc.* 1(23)

Sumer M B and Fredsøe J 2002 The mechanics of scour in the marine environment. Singapore: World Scientific

Van Rijn L C 1984 Sediment transport, part III: Bed forms and alluvial roughness. *J. Hydraul. Eng.* 110(12): 1733–1754

Whitehouse Richard (ed.) (1998) *Scour at marine structures*: *A manual for practical applications*. Thomas Telford

Wu Y and Chiew Y M 2012 Three-dimensional scour at submarine pipelines. *J. Hydraul. Eng.* 138(9): 788–795